kapin@fnal.gov

Numerical Simulations of Multipole Errors and Fringe Fields in the 1.5-TeV Muon Collider Lattice Using MADX and COSY codes

Valery Kapin* & Yuri Alexahin

(FNAL APC)

APC seminar, FNAL, Batavia, 8-Sep-2011

*G.S. at APC, on leave from “Moscow Engineering Physics Institute” (State Univ.)

The Object of the study

- Muon collider (MC) lattices with β_{IR}~1cm are featured by large β-functions and beam sizes at IR (interection region) of SC-magnets
- S.C. magnets provide essential **systematic multipolar errors**, while special constructions against muon decay products increase them
- **Fringe fields in quadrupoles** become important due to large and varying beam sizes in q-magnets at IR
- These features require to use **adequate simulation tools**
- **MADX code** is considered as an appropriate **candidate**
- The aim of the study is **to test and adapt MADX** for MC simulations
- **Modified** MADX **tracking** can **import magnet maps** from COSY code
- This work **discuss and demonstrate abilities of MADX** to be **"all-in-one" code** for MC simulations

Background for MADX usage

- MAD is a code for modeling the **beam dynamics in accelerators**.
- MAD-X is **the successor of MAD-8** (frozen in 2002).
- MAD-X offers **most of the MAD-8 functionality**.
- The most important addition is **the interface to PTC**,
  the Polymorphic Tracking Code by E. Forest (KEK, Japan).
- PTC guarantees a proper **description for thick elements**
  (arbitrary exactness with various symplectic integrators)
- MAD-X has a **modular organization** => Team:
  custodian (F.Schmidt) + Module Keepers
- **"PTC-TRACK module"** is developed by V.Kapin (ITEP) & F.Schmidt (CERN) in frames of ITEP-CERN collaboration 2004-2006

  Also high-order kicks are incorporated into to thick-magnets via MADX "PTC module" by VK & FS in 2005.
- MAD-X Home Page: http://mad.home.cern.ch/mad/"

Subjects

- Refs. on status of M.C. lattice design
- Needs for simulations of *multipole errors* and *fringe fields*
- MADX modules: abilities for simulations of multipoles errors and fringe fields
- COSY: export of magnet maps
- DA vs. fringe fields
- DA vs. sextupolar errors
- Chromaticity vs. multipole errors

- **USER'S GUIDE**
- Table of contents

EUROPEAN ORGANIZATION FOR NUCLEAR RESEARCH

M.C. lattice design and study: refs. & team

1. Yu.Alexahin, “M.C. Lattice Design Status”, M.C. workshop, Telluride CO, July, 2011 (Beams-doc-3895-v1)
2. Y.I.Alexahin, E.Gianfelice-Wendt, V.Kapin, “Chromaticity Correction for M.C. Optics”, PAC’11, New York, 2011
3. Y.I.Alexahin, E.Gianfelice-Wendt, V.Netepenko, “Conceptual Design of the M.C. Ring Lattice”, IPAC’10, Kyoto, 2010
4. Y.I.Alexahin, E.GianFelice-Wendt, V.V.Kashikin, N.V.Mokhov, A.V.Zlobin, V.Alexakhin, “M.C. Interaction Region Design”, ibid.
5. A.V.Zlobin, Y.I.Alexahin, V.V.Kashikin, N.V.Mokhov, “Magnet design for M.C. ring & IR”, ibid
6. A.Netepenko, “M.C. Lattice Design”, Beams-doc-3579-v1, 2010
7. Y.I.Alexahin, E.Gianfelice-Wendt, V.Netepenko, “New M.C. lattice design”, Beams-doc-3477-v1, 2009

MC lattice and magnet requirements [1]

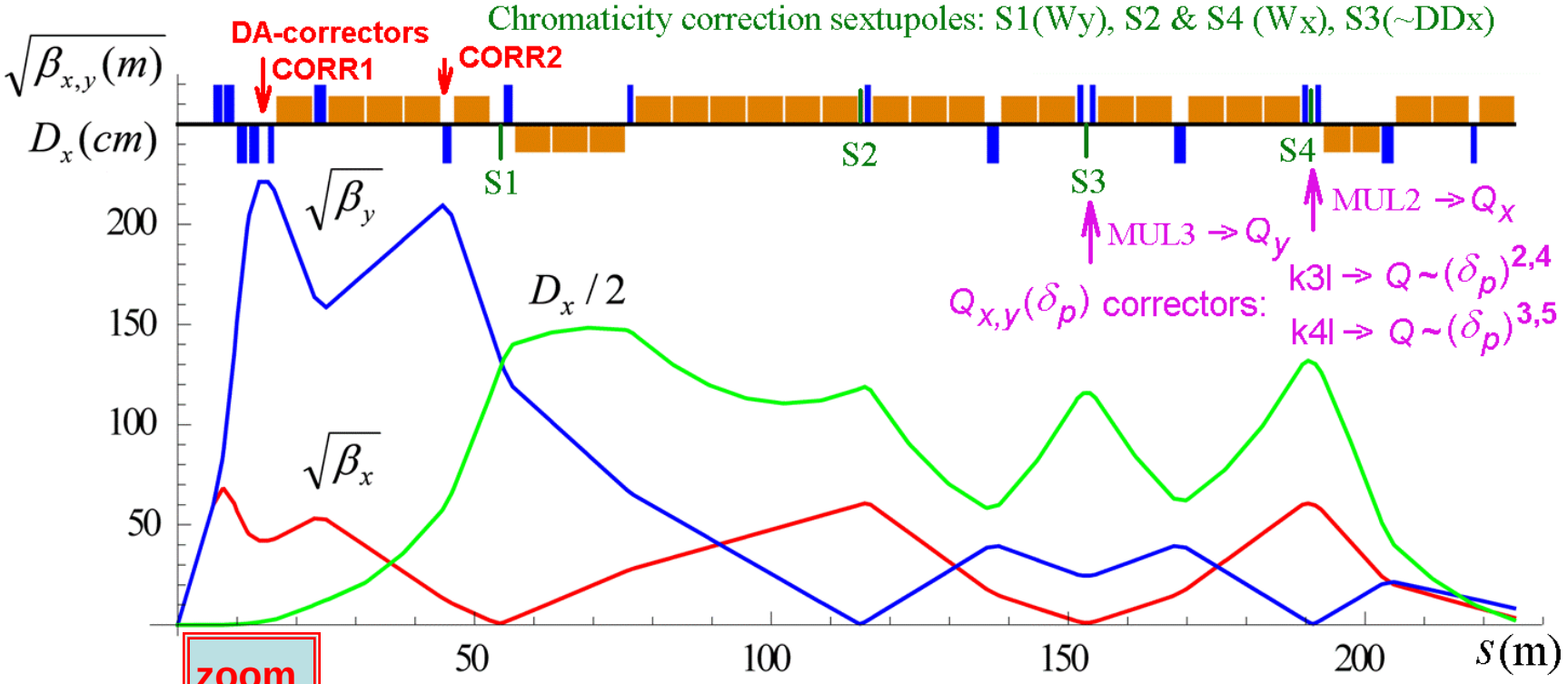

zoom

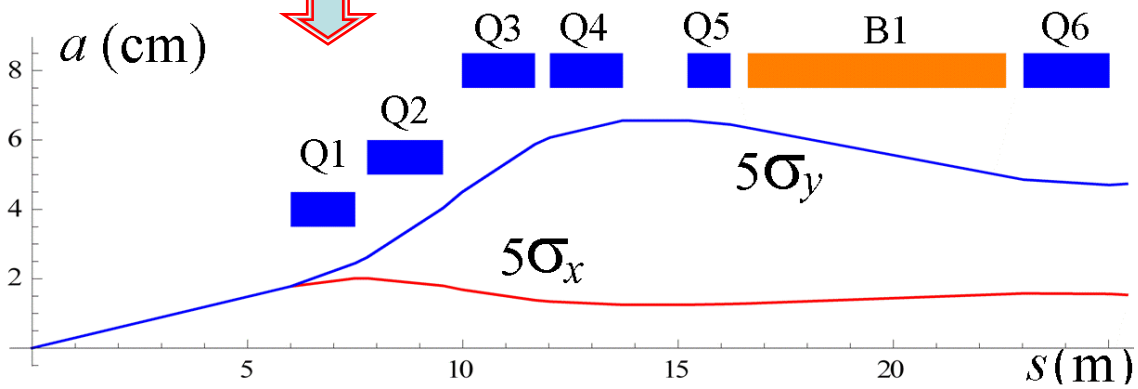

Beam energy (TeV)	0.75
IR beta-function β* (cm)	~1
Geom. r.m.s. Emitt. (nm)	3.5
Dist. (m) “IP -> 1st Q”	6 m
B in arcs (T)	8-10
Q length (m)	~2
D length	< 6

Needs for simulations of multipole errors

Cross-section and good field region of IR dipole coil of "open mid-plane design" allowing the passage of the decay electrons

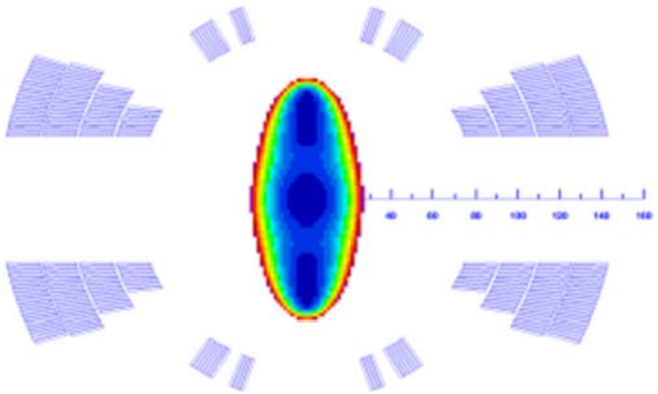

Geometrical harmonics [4,5]

R_{ref}	40mm
b_1	10^4
b_3	-5.875
b_5	-18.320
b_7	-17.105
b_9	-4.609

The standard multipole field expansion:

$$B_y(x,y)+\mathrm{i}B_x(x,y)=$$

$$=B_{ref}\times 10^{-4}\sum_{n=1}^{\infty}(b_n+\mathrm{i}a_n)\left(\frac{x+\mathrm{i}y}{r_{ref}}\right)^{n-1}$$

Relatively large values of geometrical harmonics in comparison with the traditional cos(θ) design

With MAD notation the circular multipoles are written as

$$B_y+iB_x=$$

$$=B\rho\cdot\sum_{m=0}^{\infty}\frac{\left(k_m^{\mathrm{norm}}+ik_m^{\mathrm{skew}}\right)(x+iy)^m}{m!}$$

m=0, 1, 2,… for dipole, quadr., sext., resp.

With the relation

$m=n-1,$

and at $B_{\mathrm{ref}}=8\mathrm{T},$

$(B\rho)=2500\,\mathrm{T}\cdot\mathrm{m}:$

$$k_{n-1}^{\mathrm{norm}}=3.2\cdot10^{-7}\times\frac{(n-1)!}{r_{\mathrm{ref}}^{n-1}}\cdot b_n$$

for $L=6\mathrm{m}$, the MAD kicks

$\mathrm{knl}=k_{n-1}^{\mathrm{norm}}\cdot L$:

m	knl
2	$-1.41\cdot10^{-2}$
4	$-3.30\cdot10^{+2}$
6	$-5.77\cdot10^{+6}$
8	$-5.44\cdot10^{+10}$

Needs for simulations of fringe fields in Qs

Discussion and comprehensive list of reference about fringe fields in review paper*:

- general tendency to believe that contributions from opposite ends of Qs cancel each other. It is true for most rings. Q-FF are neglected in codes, e.g. MAD8, etc.
- FF effects may be important:
  - in small rings with a large emittances (~10m·rad) and short magnets;
  - in colliders for magnets in IR, where the β-function variation is big.

Nuclear Instruments and Methods in Physics Research A 427 (1999) 74–78

The influence of fringe fields on particle dynamics in the Large Hadron Collider

Weishi Wan[a,*], Carol Johnstone[a], Jim Holt[a], Martin Berz[b], Kyoko Makino[b], Michael Lindemann[b], Béla Erdélyi[b]

[a]Fermi National Accelerator Laboratory, Beams Division, P.O. Box 500, Batavia, IL 60510-0500, USA
[b]Michigan State University and National Superconducting Cyclotron Laboratory, East Lansing, MI 48824, USA

the use of high-gradient quadrupoles in the interaction region.
quadrupoles combine relatively short length, large aperture, short focal length,
all of which enhances the relevance of their fringe field effects.
the code COSY INFINITY differential algebraic (DA)
An analysis reveals that the strength of resonances increases and
amplitude-dependent tune shifts are enhanced substantially.

* Y.Papaphilippou, J.Wei, R.Talman, “Deflections in magnet fringe fileds”, PR-E67, 2003

QFF simulations: approaches

Fig. 1. Illustration of possible variations of the function $k(z)$
The rectangle BCC′B′ in (a) gives the rectangular model.
The linear-ramp model is illustrated in part (c).

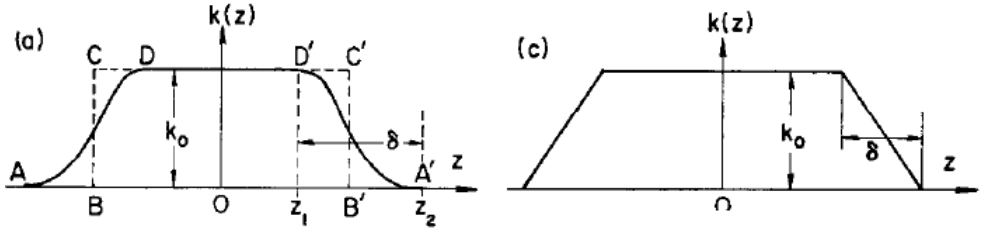

Old studies for QFF formulae:
K.Steffen (1965 - book),
G.E. Lee-Whiting (1970)
D.L. Smith (1970)
H.Wollnik (1970, 1972),
P.Krejcik (1987),
S.Koscielniak (2007), …

For segments of rapidly varying $k(z)$ the problem is more difficult.

Using subscripts 1 and 2 for the beginning and end of a segment we may write

$$x_2 = M_{11}x_1 + M_{12}x_1' + \Delta x,$$
$$x_2' = M_{21}x_1 + M_{22}x_1' + \Delta x'.$$

Δx is the third-order part

Lee-Whiting[a]

In the limit $z_2 \to z_1$ we have for the transition from $k = 0$ to $k = k_0$:

$$\Delta x = \left[\tfrac{1}{12}x_1^3 + \tfrac{1}{4}x_1 y_1^2\right] k_0, \qquad (8a)$$
$$\Delta x' = \left[\tfrac{1}{2}x_1 y_1 y_1' - \tfrac{1}{4}x_1'(x_1^2 + y_1^2)\right] k_0. \qquad (8b)$$

Symplectic maps for FF:
1) E.Forest (1988 book -> PTC)
2) M.Berz & H.Wollnik (1990) -> M.Berz & Co. (1990 -> present)

a) G.E. Lee-Whiting, “Third Order Aberations of a Magnetic Quadrupole Lens”, NIM-83, pp.232-244 (1970)

Symplectic maps for QFF

E.Forest, “Beam Dynamics: a new attitude and framebook”, 1998.

$$x^f = x \pm \frac{b_2}{12(1+\delta)}\{x^3 + 3y^2x\} \quad (13.33.a)$$

$$p_x^f = p_x \pm \frac{b_2}{4(1+\delta)}\{2xyp_y - x^2p_x - y^2p_x\} \quad (13.33.b)$$

$$y^f = y \mp \frac{b_2}{12(1+\delta)}\{y^3 + 3x^2y\} \quad (13.33.c)$$

$$p_y^f = p_y \mp \frac{b_2}{4(1+\delta)}\{2xyp_x - y^2p_y - x^2p_y\} \quad (13.33.d)$$

$$\delta^f = \delta \quad (13.33.e)$$

$$\ell^f = \ell - \frac{f_\pm}{(1+\delta)}. \quad (13.33.f)$$

390 FRINGE EFFECTS IN RING DYNAMICS

13.2.3 A Famous Case: Lee-Whiting's Quadrupole Map

The results presented here for the straight elements were first derived by Milutinovic[67] and the author. However the most important application, the quadrupole fringe field map, was first correctly derived by Lee-Whiting in a paper on quadrupole fringe effects. Lee-Whiting took the hard-edge limit of his more complex formulas just out of curiosity. He never really expected this limit to be of any use. The reader should remember our discussion about the contrast between single pass systems and rings: their demands on absolute accuracy are usually much higher and certainly very different.

PTC lib. by E.Forest implements the above “Lee-Whiting’s HE-limit” formulae for QFF .

M.Berz, K.Makino, B.Erdelyi, “Magnet Fringe Fields, ..”, PAC’2001.

Details on COSY’s QFF comes in next slides

3 FRINGE FIELD EFFECTS

For simulations of large storage rings, fringe field effects are often neglected. Even though sometimes this is a quite good approximation, strictly speaking, it is an unphysical model, as the electromagnetic fields of the model do not satisfy Maxwell's equations. The simplest method to take fringe fields into account is to take their effect with a kick characterized by the integrated field value [12], but more sophisticated models are needed for accurate simulations. Refer to [4] for the detailed discussion on the sharp cut-off approximation, and various studies on fringe field treatments. In the map picture using Differential Algebraic methods [13, 14, 15], the fringe field effects can be particularly easily studied. The fringe field effects influence all orders of the motion, beginning with the linear behavior, and the complete treatment to any order is possible in the code COSY INFINITY [8, 9, 10].

[12] G. Lee-Whiting, Nuclear Instruments and Methods, 1970.

[4] M. Berz, B. Erdélyi, and K. Makino, “Fringe Field Effects in Small Rings of Large Acceptance”, Physical Review ST-AB, 3:124001, 2000.

[15] M. Berz, “Modern Map Methods in Particle Beam Physics”, Academic Press, San Diego, 1999.

[8] M. Berz, “Computational Aspects of Design and Simulation: COSY INFINITY”, Nuclear Instruments and Methods, A298:473, 1990.

[10] M. Berz, “COSY INFINITY Version 8 Reference Manual”, Technical Report MSUCL-1088, National Superconducting Cyclotron Laboratory, Michigan State University, East Lansing, MI 48824, USA, 1997. See also http://cosy.nscl.msu.edu.

[20] F. Zimmermann, C. Johnstone, M. Berz, B. Erdélyi, K. Makino, and W. Wan, “Fringe Fields and Dynamic Aperture in Muon Storage Rings”, Technical Report 95, Muon Collider Collaboration, BNL, 2000.

MADX modules: abilities for simulations of multipoles errors and fringe fields

MADX consist of two type of modules:

a) traditional modules with the most of MAD-8 functionality;

b) PTC modules as **an interface to PTC** library by E.Forest

Relevant "traditional" modules

- Twiss module (tunes, chromaticity, Wx,y, etc)
- THINTRACK via MAKETHIN
  (tracking in "KICK-DRIFT" lattice)
- SODD (Second Order Detuning and Distortion)
  as extension by FS

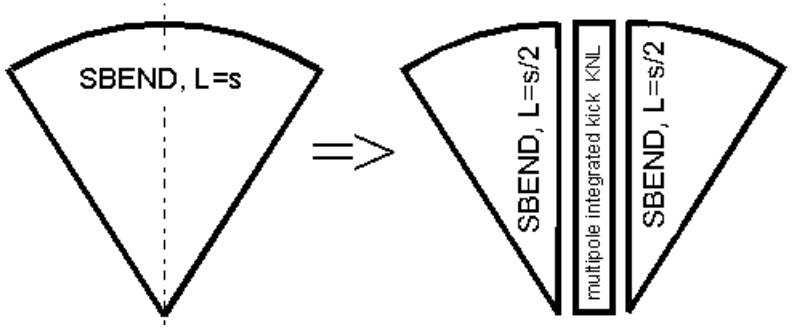

Multipole errrors in thick magnet via splitting;

Fringe fields in quadrupoles are absent (FFQ is not an octupole!)

PTC modules:

- PTC Set-up Parameters
- PTC_TWISS (Ripken Optics, w/o Wx,y)
- PTC-TRACK (Thick-Lens Tracking)
- PTC_NORMAL (Non-Linear Machine Parameters)

```
BE1: RBEND, l=0.2, ANGLE=0.1,
 knl:={0,0,-1.4E-02,0,-3.3E+02};
```

Multipole errors in thick magnet are incorporated (available to all modules)

"LW-HE" FF in Qs can be switched ON (by MADX source code modification)

FFQ extension via export of Quad. map from COSY INFINITY

"COSY INFINITY 9.0 Beam Physics Manual":

- Maps can be printed to ext. file with command **PM**;
- Command "**FR <mode>"** invokes fringe field computations
- Maps for general elements from measurements are also possible (!);

FR 3 & FR 2.9 **3.3.7 Fringe Fields**

This mode is the most accurate fringe field mode. The fringe field falloff is based on the standard description of the s-dependence of multipole strengths by a six parameter Enge function. The Enge function is of the form

$$F(z) = \frac{1}{1 + \exp(a_1 + a_2 \cdot (z/D) + ... + a_6 \cdot (z/D)^5)},$$

where z is the distance perpendicular to the effective field boundary. In the case of multipoles, the distance coincides with the arc length along the reference trajectory. D is the full aperture (i.e., in case of multipoles $D = 2 \cdot d$) of the particle optical element, and a_1 through a_6 are the Enge coefficients.

	a_1	a_2	a_3	a_4	a_5	a_6
Dipole	0.478959	1.911289	-1.185953	1.630554	-1.082657	0.318111
Quadrupole	0.296471	4.533219	-2.270982	1.068627	-0.036391	0.022261
Sextupole	0.176659	7.153079	-3.113116	3.444311	-1.976740	0.540068

COSY Enge coefficients by default. based on measured data from PEP at SLAC

a_1	a_2	a_3	a_4	a_5	a_6
−0.003183	1.911302	0.00	0.00	0.00	0.00
0.00004	4.518219	0.00	0.00	0.00	0.00
−0.000117	7.135786	0.00	0.00	0.00	0.00

Table 2: Enge coefficients for a simple model.

Modification of MADX "PTC-TRACK" done by VK allows to import externally generated map and use in particle tracking (ELEMENT_BY_ELEMENT):

STEPS: testing and understanding COSY maps for Qs; coordinate transformation COSY-> MADX; subroutines for reading and calculating maps; testing runs)

Particle tracking with PTC_TRACK

All w/o FFQ and multipole errors

Phase space trajectories at x_0=0

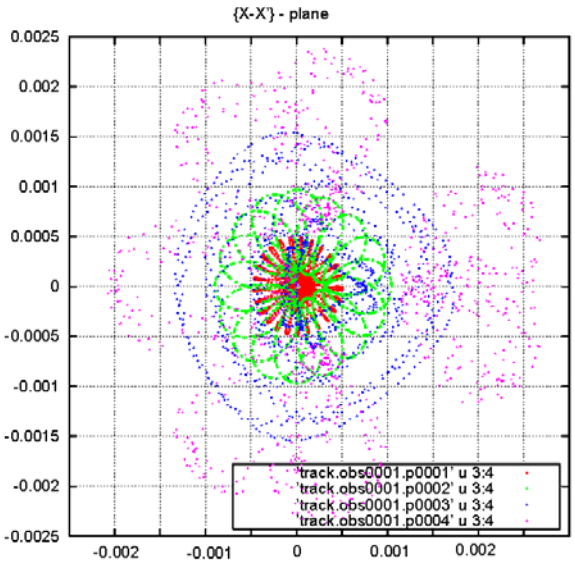

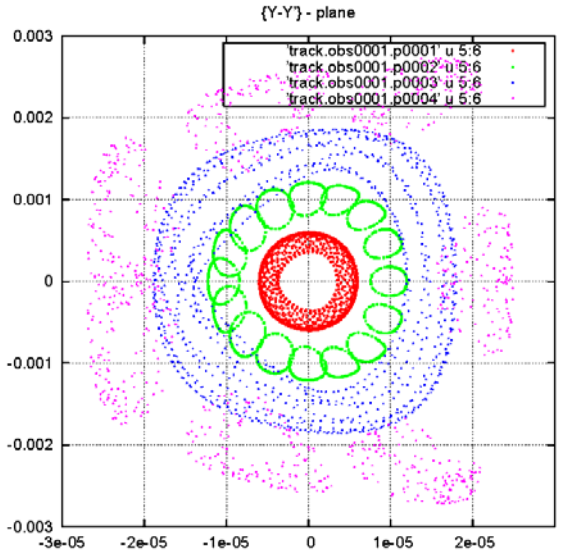

y_0=6; 12; 18 24μm

Phase space trajectories at x_0=6μm

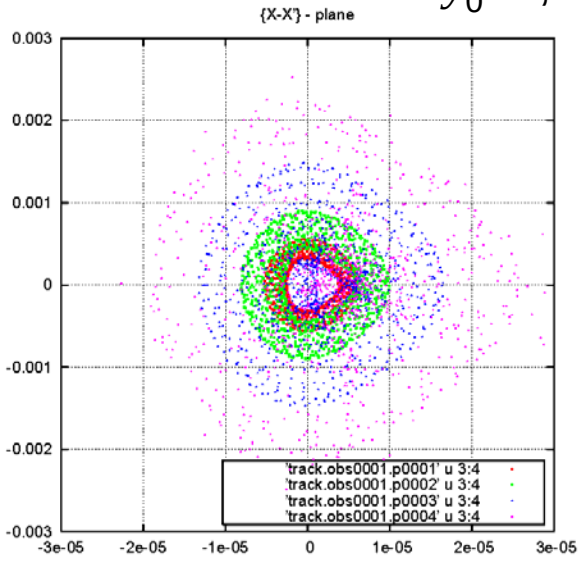

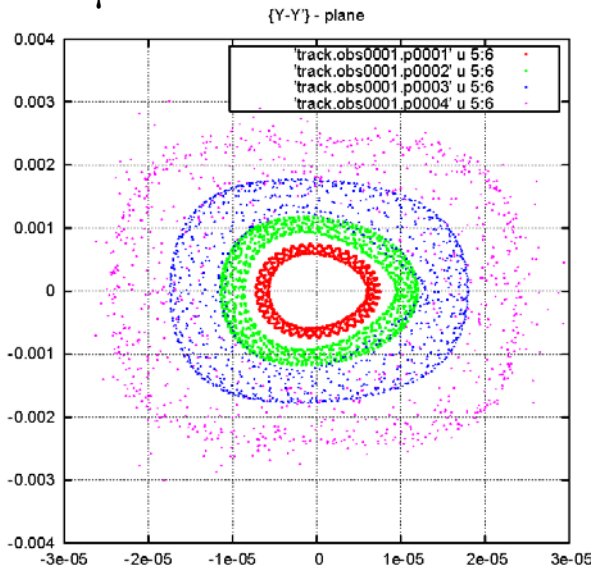

strong non-linear coupling

DA vs. fringe fields

Tracking results using modified PTC-TRACK

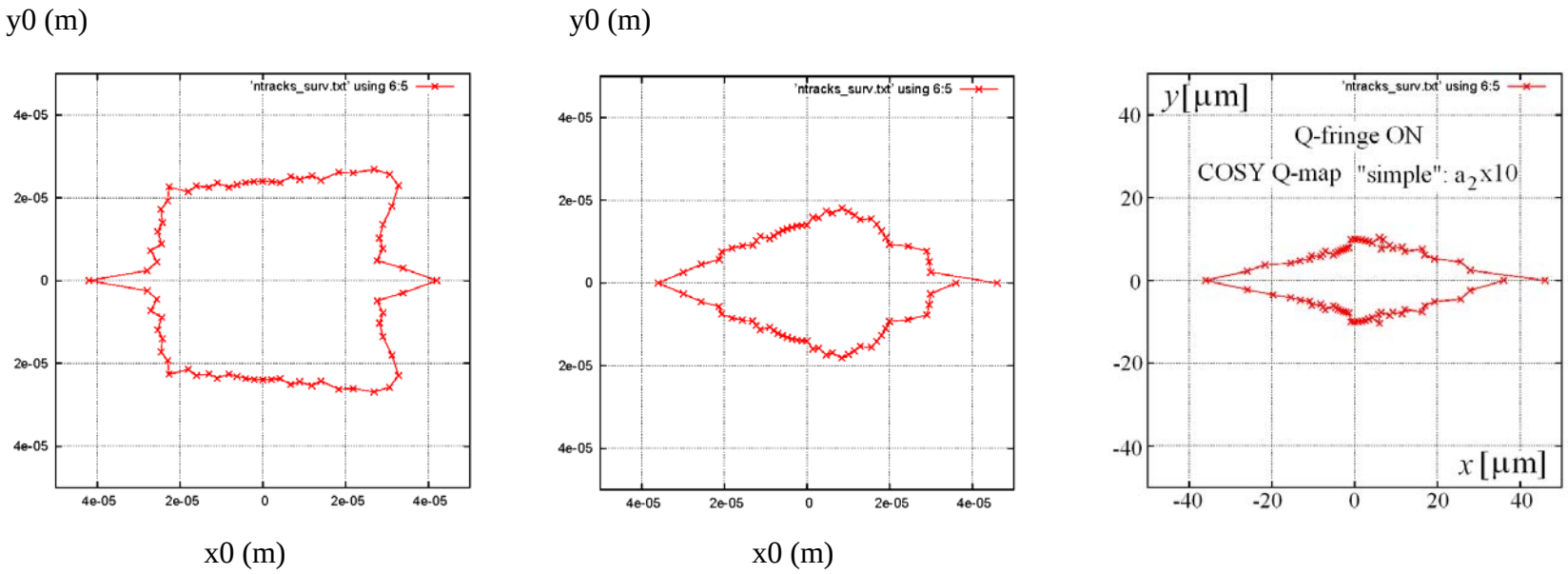

1000 turns DA for 1.5TeV lattice in units of initial coordinates at IP (x'=y'=0):

without (left) and with quadrupole fringe fields: center - embedded in MAD-X PTC hard-edge approximation, right - maps produced by COSY.

- **Only vertical motion suffers due to βy_max>> βx_max**
- **PTC underestimates the effect**

DA vs mutipole errors: detuning coefficients

Detuning coefficients ("tune shifts vs. amplitude") are helpful for DA optimization:
An increase in detuning coefficients leds to to DA reduction

Two procedures for det. coeff. calculations are used:
a) PTC_NORMAL b) TBT analysis of PTC_TRACK data

Parameter		ptc_norm		track 2^10 (**1024**) (tbt: 1/N2)										Netepenko
nst, no (N-forms)		~~10 (~as1), exact, no=6~~	10(as~1), exact, no=5,6	nst=1, exact uniform mesh on X-Y plane "10-2ord //6-2ord" points or "…/…/10-3ord"										
Nturns				64		128		256		512		1024		
step on (X-Y)				h=3mkm										
				w/o I-aver	with I-aver	w/o I-aver	with I-aver	w/o I-aver	with I-aver	w/o I-aver	with I-aver	w/o I-aver	with I-aver	
qx	by twiss	18.560000		.5599935/ .5600039/ .5600043	.5599959/ .5600040/ .5600043	.5599973/ .5600007/ .5600007	.5599977/ .5600007/ .5600008	.5599984/ .5600103/ .5600109	.5599992/ .5600104/ .5600109	.5599691/ .5599542/ .5599537	.5599695/ .5599543/ .5599534	.5600264/ .5599904/ .5599889	.5600264/ .5599905/ .5599889	
			0.56											
qy	by twiss	18.550000		.5500534/ .5499969/ .5499945	.5500568/ .5499969/ .5499945	.5499953/ .5500032/ .5500035	.5499965/ .5500032/ .5500035	.5500012/ .5499981/ .5499981	.5500032/ .5499982/ .5499980	.5500020/ .5499912/ .5499909	.5500020/ .5499912/ .5499908	.5499736/ .5499880/ .5499887	.5499756/ .5499880/ .5499886	
	by ptc-normal		0.55											
$\partial Q_x/\partial\varepsilon_x$	*-2.63e05*		-2.530e05	-2.6/-2.6/ -2.5 E5	**-2.6/-2.6/ -2.6 E5**	**-2.5/-2.5/ -2.5 E5**	**-2.5/-2.5/ -2.5 E5**	-2.5/-2.7/ -2.8 E5	-2.5/-2.8/ -2.8 E5	-2.4/-2.2/ -2.2 E5	-2.4/-2.2/ -2.2 E5	-3.2/-2.6/ -2.5 E5	-3.2/-2.6/ -2.5 E5	-1.2e+5*2= **-2.4E+5**
$\partial Q_x/\partial\varepsilon_y$	*1.27e5*		+1.071e05	+6.7/+3.9/ +3.5 **E4**	+5.3/+3.4/ +3.1 **E4**	**+1.2/+1.1/ +1.1 E5**	**+1.1/+1.1/ +1.1 E5**	+1.2/+1.1/ +1.0 E5	+1.1/+1.0/ +1.0 E5	+1.2/+1.5/ +1.6 E5	+1.2/+1.5/ +1.6 E5	+1.02/+1.3/ +1.3 E5	+0.90/+1.2/ +1.3 E5	(+9.4e+4) *2=**1.88e+5**
$\partial Q_y/\partial\varepsilon_x$	*1.27e5*		+1.071e05	-9.9/+2.5/ +5.0 **E4**	-1.0/+0.3/ +0.5 **E5**	**+1.2/+1.0/ +1.0 E5**	**+1.2/+1.0/ +1.0 E5**	+0.8/+1.0/ +1.0 E5	+0.9/+1.0/ +1.0 E5	+0.7/+1.1/ +1.2 E5	+0.7/+1.1/ +1.2 E5	+0.6/+1.2/ +1.2/ E5	+1.2/+1.2/ +1.2 E5	
$\partial Q_y/\partial\varepsilon_y$	*-2.39e5*		+1.487e05	+1.4/+1.5/ +1.5 E5	+1.4/+1.5/ +1.5 E5	**+1.4/+1.5/ +1.5 E5**	**+1.5/+1.5/ +1.5 E5**	+1.5/+1.5/ +1.5 E5	+1.5/+1.5/ +1.5 E5	+1.5/+1.3/ +1.3 E5	+1.5/+1.3/ +1.3 E5	+1.7/+1.3/ +1.2 E5	+1.7/+1.3/ +1.3 E5	-1.5e+5*2= **-3.0E+5**
$\partial^2 Q_x/\partial\varepsilon_x^2$	*-6.68e10*		-6.08e10	+2.1/+0.4/ +0.02 E12	+1.0/+0.2/ +0.3 E12	+3.1/**-0.6**/ -0.9 E11	-5.0/-1.8/ -4.0 E11	+0.1/+0.8/ +1.4 E13	+0.04/+0.8/ +1.5 E13	-0.2/-0.7/ -1.2 E13	-0.2/-0.8/ -1.3 E13	+1.5/-1.0/ -3.3 E13	+1.4/-1.1/ -3.4 E13	
$\partial^2 Q_x/(\partial\varepsilon_x\partial\varepsilon_y)$	*4.97e14*		+7.173e12	-6.0/-6.6/ -8.3 E12	-1.3/-1.4/ -1.6 E13	+7.3/+7.1/ +6.4 E12	+8.4/+6.7/ +4.3 E12	+0.7/+1.6/ +2.4 E13	+0.9/+1.8/ +2.5 E13	+0.8/-1.1/ -2.8 E13	+1.0/-1.2/ -3.2 E13	+2.5/+1.6/ +1.1 E13	+3.0/+1.7/ +0.7 E13	
$\partial^2 Q_x/\partial\varepsilon_y^2$	*-5.05e14*		-1.222e13	-3.4/-2.4/ -1.7 E13	-3.0/-2.3/ -1.8 E13	-1.6/-1.3/ -1.1 E13	-1.4/-1.3/ -1.1 E13	-1.7/-1.2/ -0.9 E13	-1.5/-1.2/ -0.9 E13	-1.7/-2.7/ -3.7 E13	-1.6/-2.7/ -3.7 E13	-1.4/-2.0/ -2.3 E13	-1.2/-2.0/ -2.4 E13	
$\partial^2 Q_y/\partial\varepsilon_x^2$	*4.97e14*		+7.173e12	+2.8/-2.0/ -6.0 E13	+2.9/-2.1/ -6.1 E13	+1.0/+1.7/ +2.2 E13	+1.1/+1.7/ +2.2 E13	+1.7/+1.4/ +1.1 E13	+1.7/+1.4/ +1.1 E13	+1.9/+0.4/ -0.9 E13	+2.0/+0.4/ -0.9 E13	+1.1/+1.0/ +0.8 E13	+1.2/+1.0/ +0.8 E13	
$\partial^2 Q_y/(\partial\varepsilon_x\partial\varepsilon_y)$	*-5.05e14*		-1.222e13	-1.2/-2.0/ -2.1 E13	-0.8/-1.6/ -1.7 E13	-2.0/-2.2/ -2.4 E13	-1.5/-1.4/ -1.3 E13	-1.8/-1.6/ -0.1 E13	-1.2/-0.7/ -0.1 E13	-1.3/-0.9/ -0.5 **E13**	-6.2/+0.4/ +6.6 **E12**	-2.5/-1.7/ -1.1 E13	-2.0/-0.8/ +0.2 E13	
$\partial^2 Q_y/\partial\varepsilon_y^2$	*-1.61e12*		-2.825e12	-1.3/-1.1/ -0.8 E12	-1.7/-2.5/ -2.9 E12	-1.1/-1.5/ -1.8 E12	-2.6/-3.2/ -3.7 E12	-1.9/-0.9/ +0.01 E12	-3.2/-2.5/ -1.9 E12	-0.2/+0.6/ +1.4 E13	-0.3/+0.4/ +1.1 E13	-0.6/+0.9/ +2.2 E13	-0.7/+0.7/ +1.9 E13	

Correction sextupole error by sextupole of CORR1 via ptc_normal and TBTof PTC-TRACK

PTC_NORMAL reproduce
Parabolic dependence on
Sext. Strength k2nl

Opt.K2nl ~-0.02

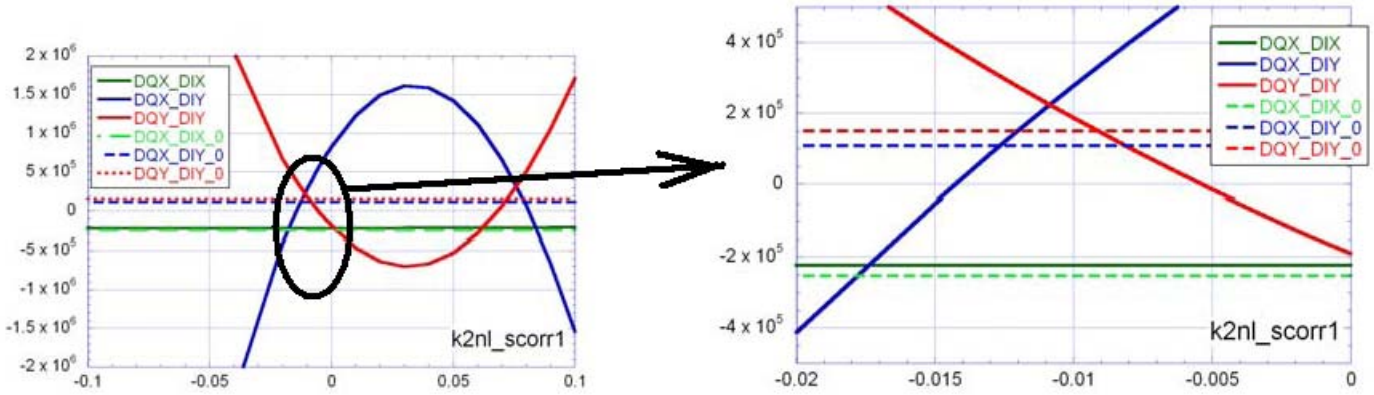

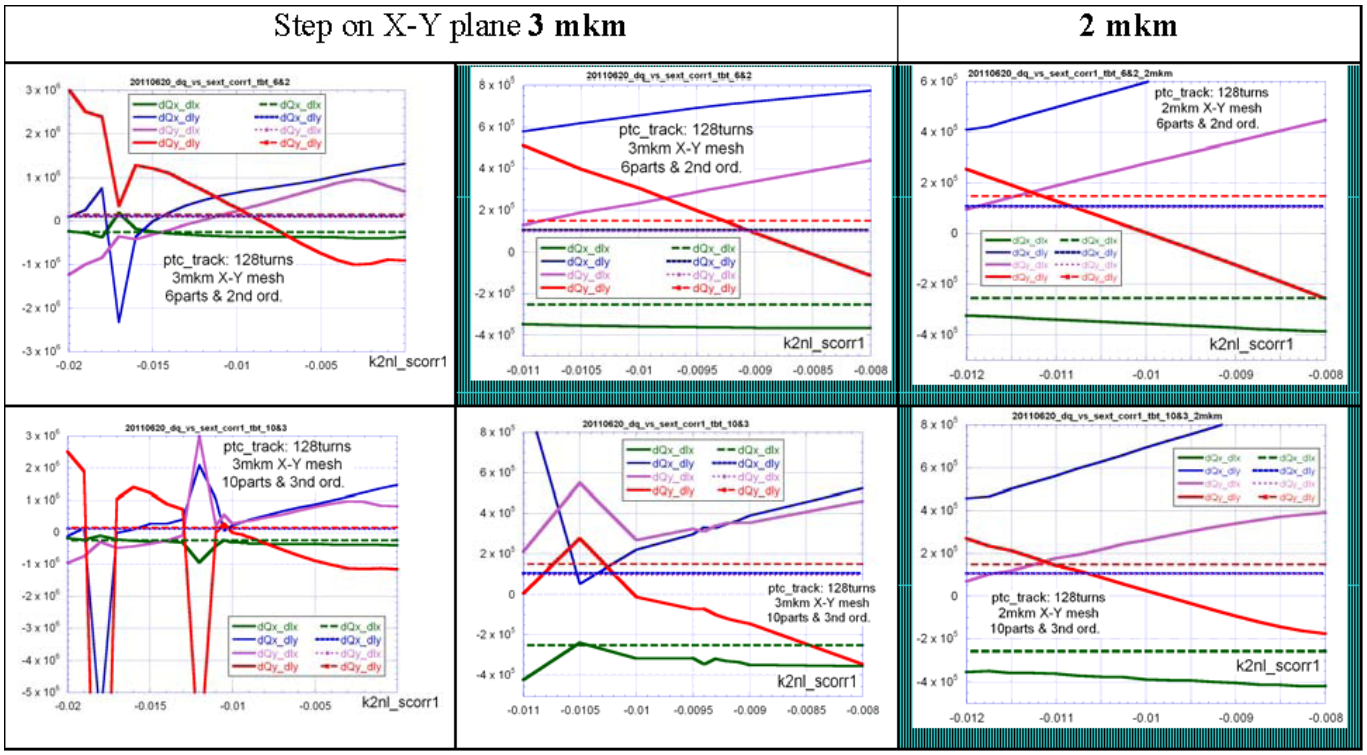

TBT of PTC_TRACK
Reproduce noisy
Parabolic dependences

Opt.K2nl ~-0.01

DA vs mutipole errors: optimization via scanning k2nl

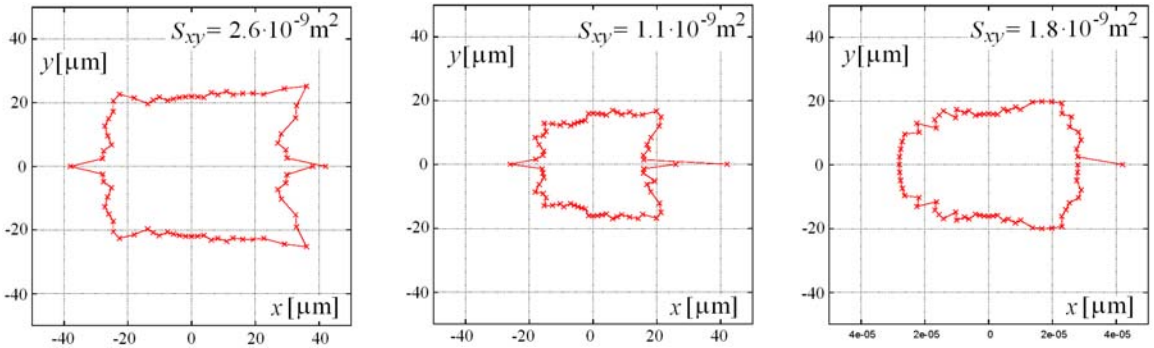

DA in the plane of initial particle coordinates:. left - no multipole errors, center - sextupole error added, right - sextupole corrector placed at the 1st βy maximum.

- **Effect of the sextupole error can also be compensated with octupole (Netepenko)**
- **Sextupole error affects both x- and y-motion**

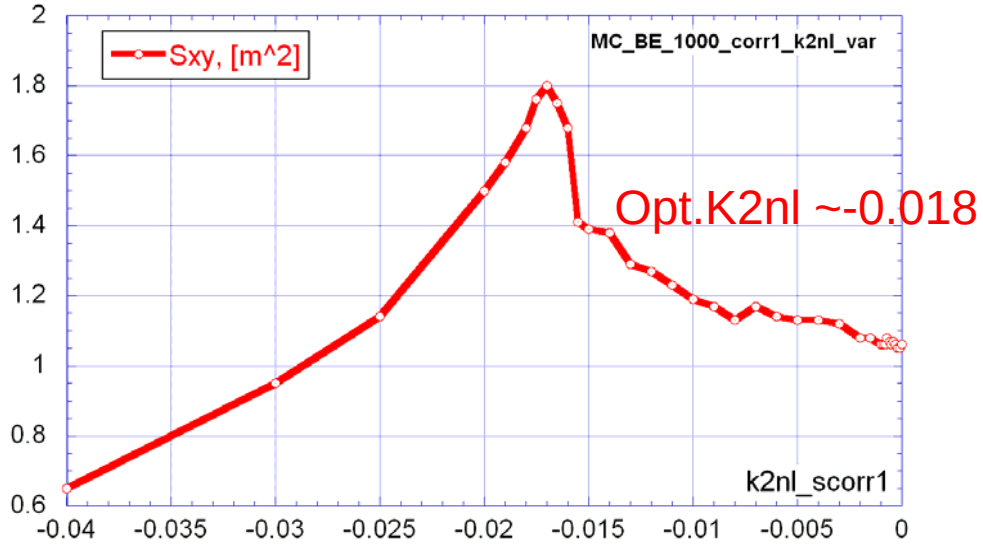

Optimistic results for CORR2

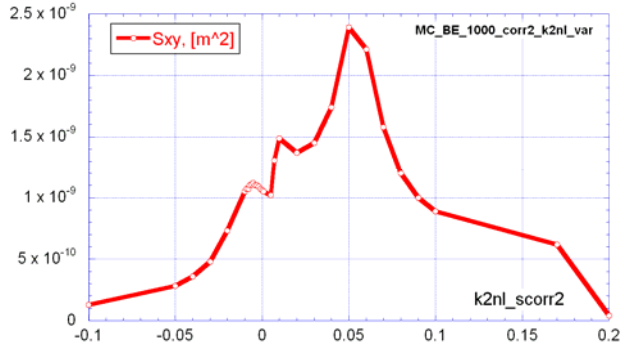

All multipole errors of IR Dipoles

Effect of multipole components on DA in 1.5TeV case: decapole is most detrimental

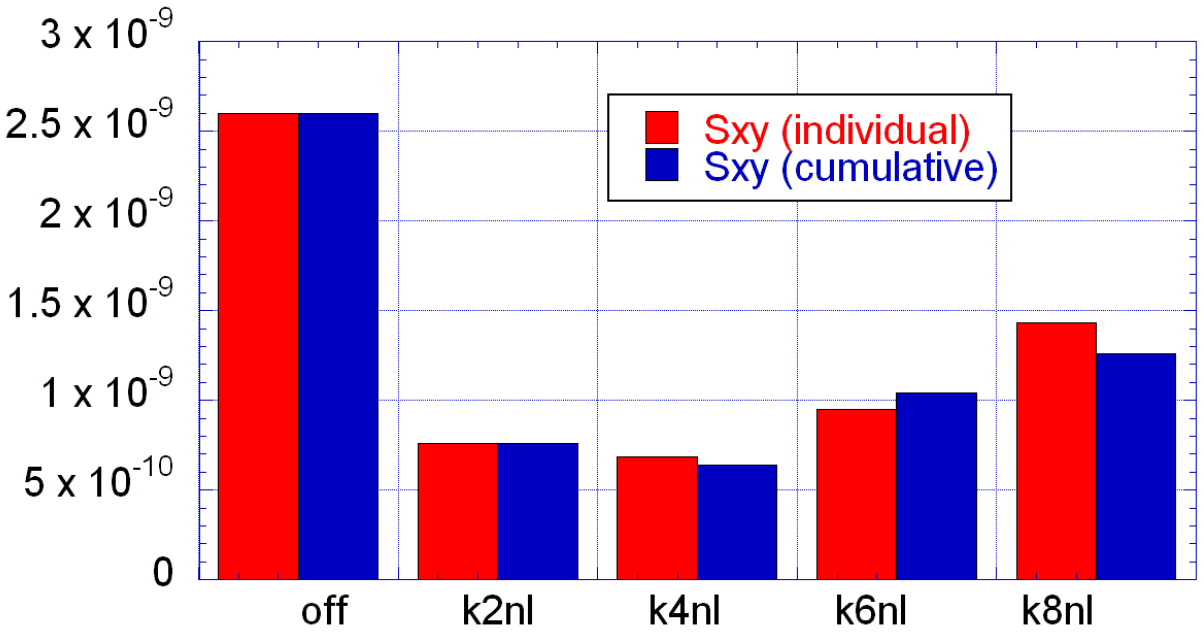

"Head-on" attempts to maximize DA (at all multipole errors) by simple scanning of every multipole k*nl of CORRs are not succesfull.

=> Needs for nonlinear corrector arrangements for multipole error correction

Chromaticity corrections with TWISS module (traditional MADX)

Lattice preparations

Magnet conversion (slicing) for traditional MADX: a) BE1: rbend; b) BE1: sbend; c) BE1: sbend splitted onto 5 segmens; d) 5 sextupoles k2l are on in BE1.

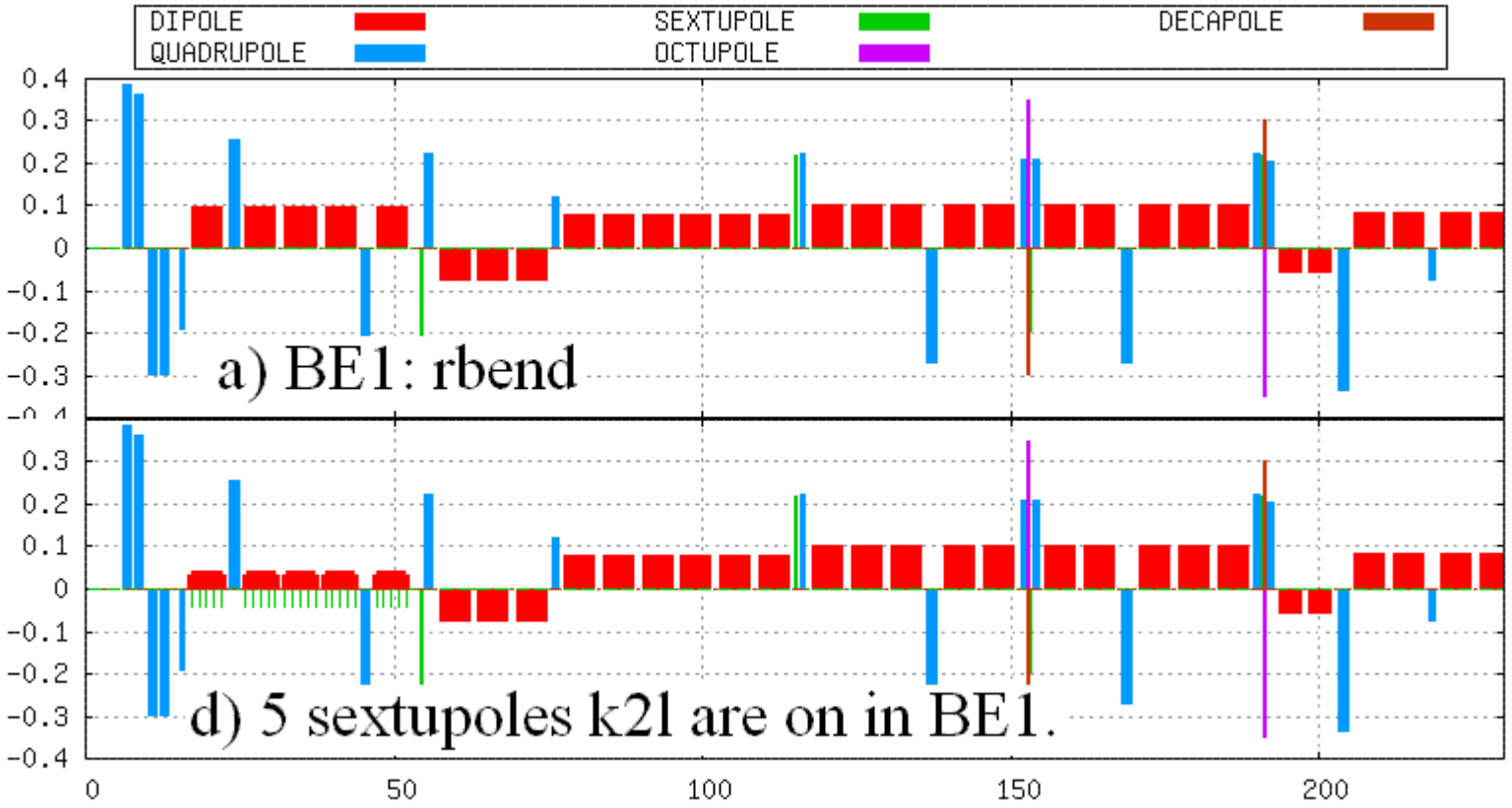

Chromaticity corrections with TWISS module

Montague chromatic functions:

"a) up to c)" – no differences; d) 5 sextupoles k2l are ON in BE1.

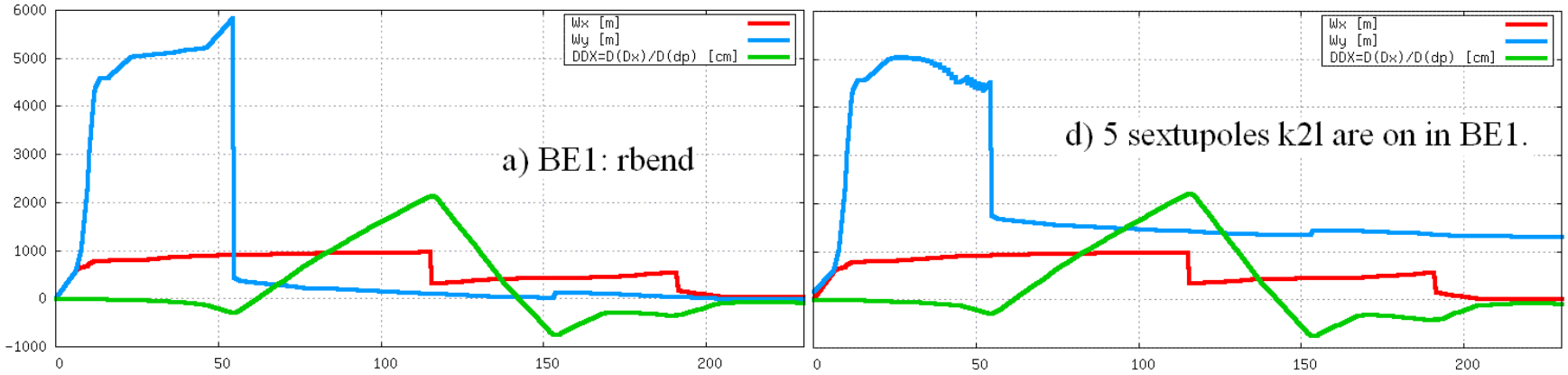

Matching constraints study:
Matching results are the same for both Wy and DQ2

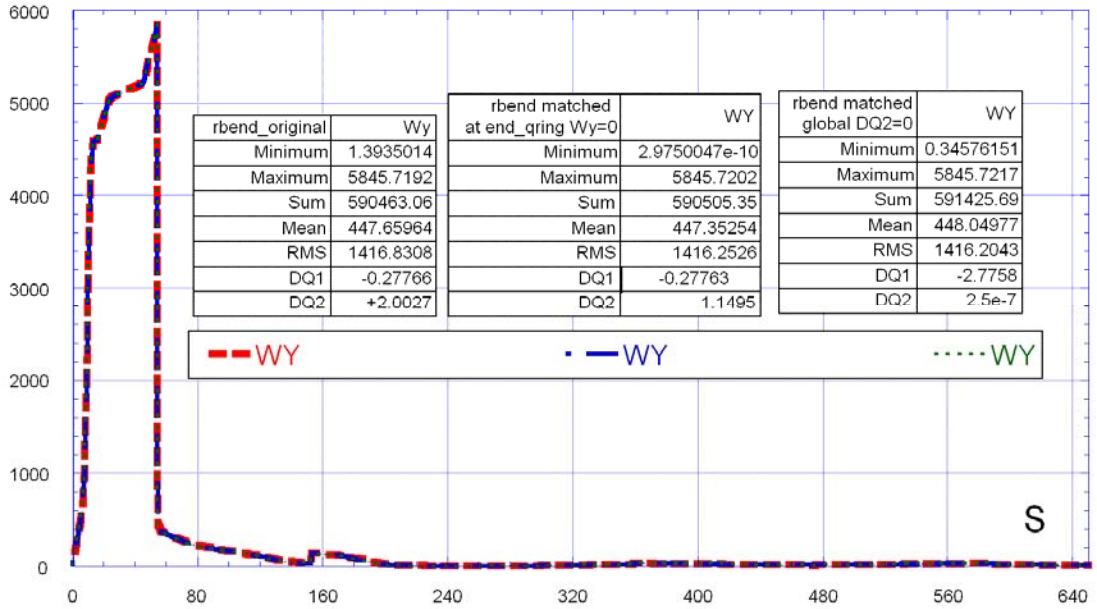

rbend_original	Wy
Minimum	1.3935014
Maximum	5845.7192
Sum	590463.06
Mean	447.65964
RMS	1416.8308
DQ1	-0.27766
DQ2	+2.0027

rbend matched at end_qring Wy=0	WY
Minimum	2.9750047e-10
Maximum	5845.7202
Sum	590505.35
Mean	447.35254
RMS	1416.2526
DQ1	-0.27763
DQ2	1.1495

rbend matched global DQ2=0	WY
Minimum	0.34576151
Maximum	5845.7217
Sum	591425.69
Mean	448.04977
RMS	1416.2043
DQ1	-2.7758
DQ2	2.5e-7

Chromaticity corrections with TWISS module

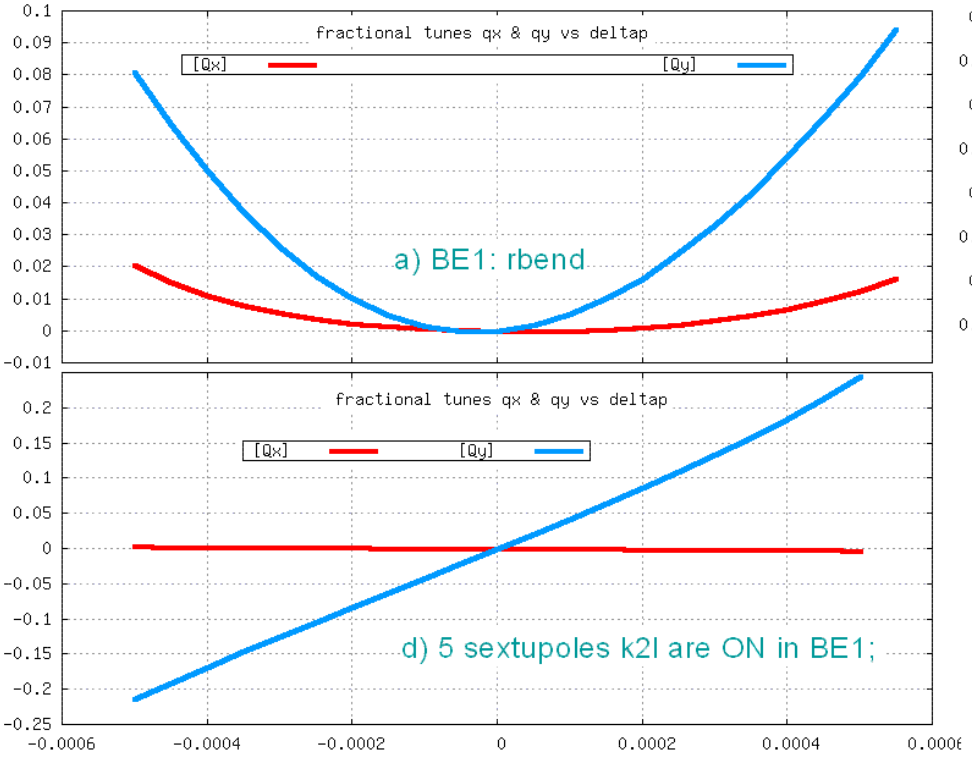

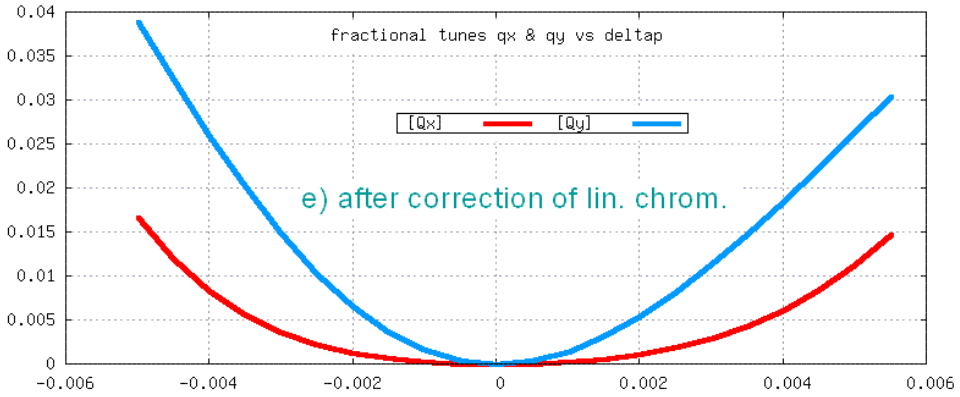

Tunes vs deltap:
a) BE1: rbend;
d) 5 sextupoles k2l are ON in BE1;
e) after correction of liner chromaticity with MADX matching commands.

Non-linear chromaticity corrections with TWISS module

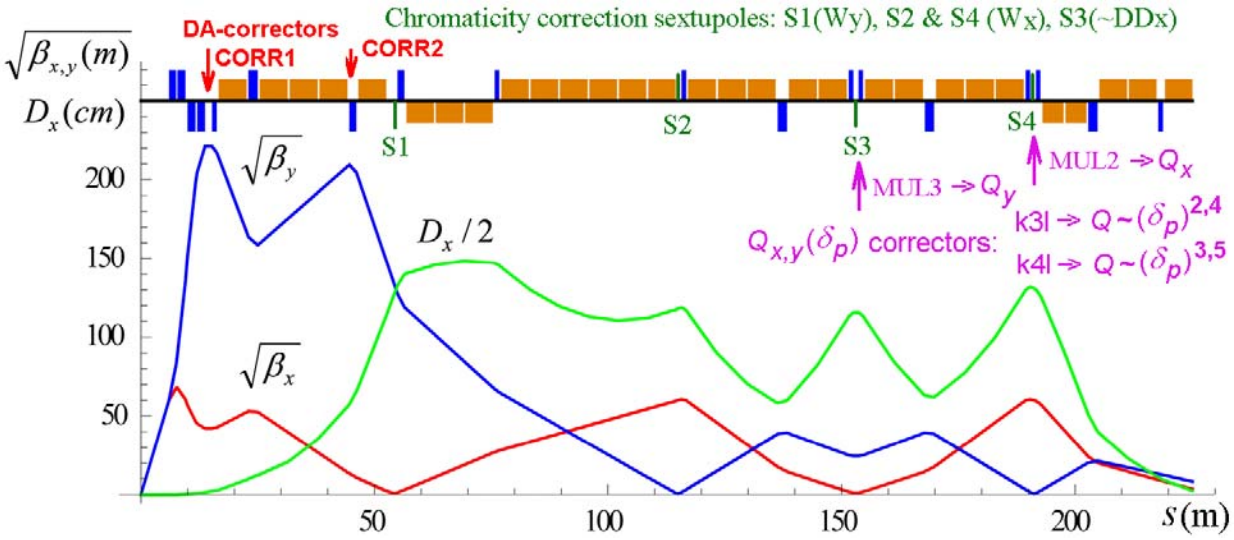

Final plot with Twiss

All multipoles in BE1 are on

It is helpful to use ploting software which provides polinomial fitting coefficients

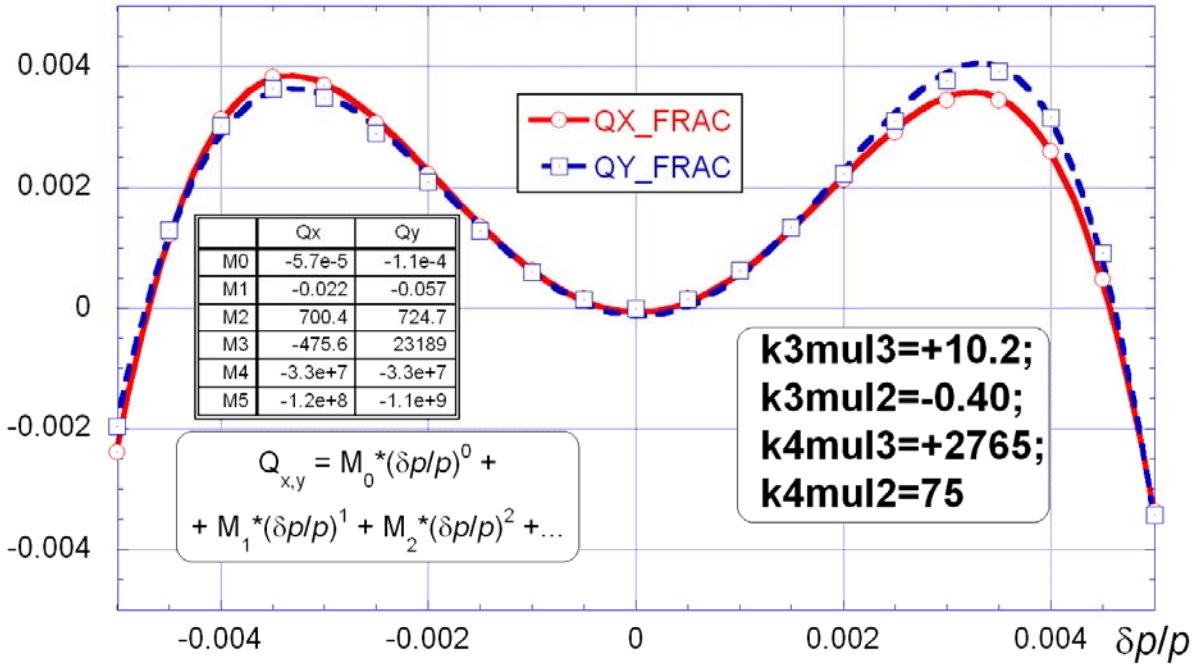

Non-linear chromaticity corrections: TWISS -> PTC_TWISS

Transfer to PTC_TWISS:

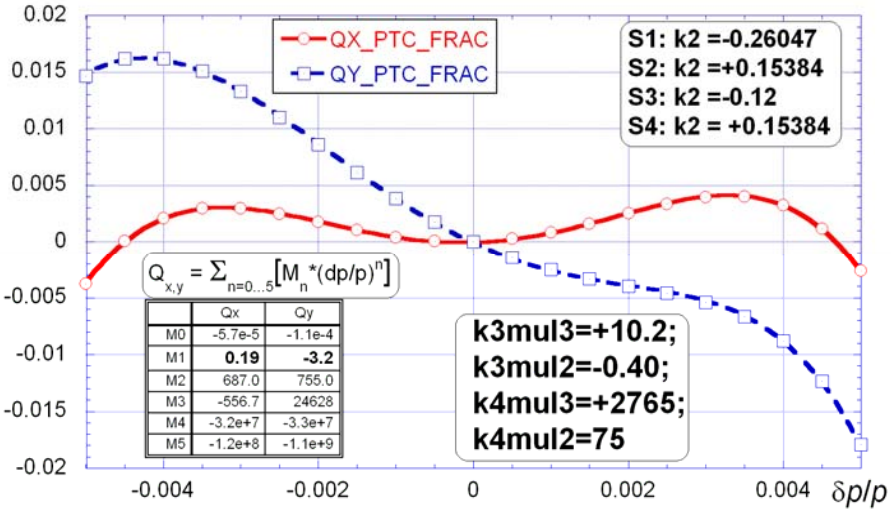

	Qx	Qy
M0	-5.7e-5	-1.1e-4
M1	**0.19**	**-3.2**
M2	687.0	755.0
M3	-556.7	24628
M4	-3.2e+7	-3.3e+7
M5	-1.2e+8	-1.1e+9

Small tuning by linear chrom. correctors S1& S2-4:

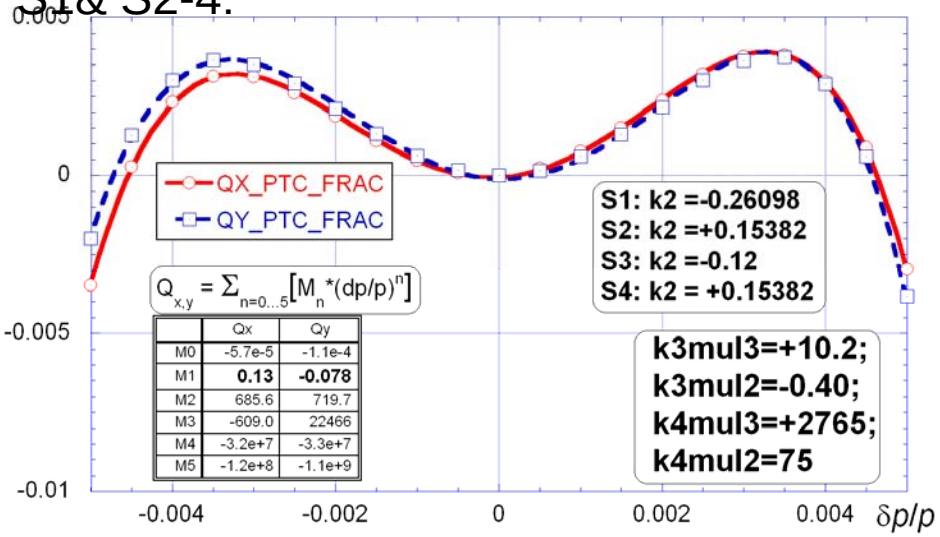

	Qx	Qy
M0	-5.7e-5	-1.1e-4
M1	**0.13**	**-0.078**
M2	685.6	719.7
M3	-609.0	22466
M4	-3.2e+7	-3.3e+7
M5	-1.2e+8	-1.1e+9

Plots for the range of $\delta p = \pm 0.6\%$

$\Delta Qx,y \in$ [-0.018;+0.004]
[-0.022;+0.004]

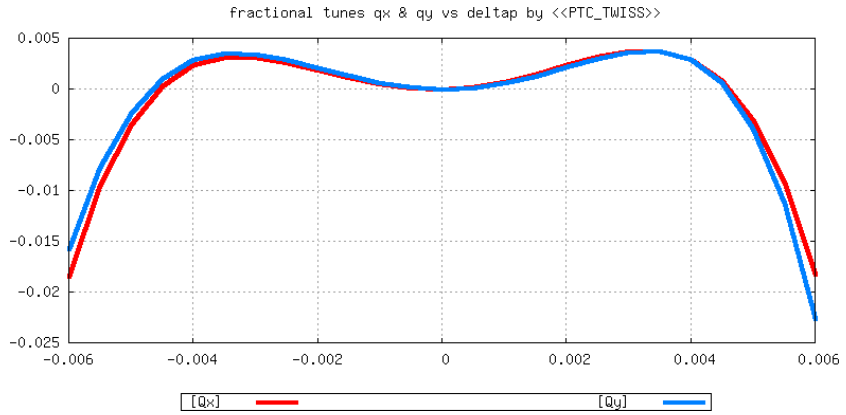

Conclusions

- Muon collider (MC) lattice requires simulations with adequate treatments of **systematic multipolar errors and Fringe fields in quadrupoles**
- **MADX code with relevant extensions and modifications** can be an appropriate **candidate** to be **“all-in-one” code** for MC simulations
- **Combination MADX with COSY** as a map provider may cover most of types of quadrupole fringe fields formulations
- MADX modules TWISS, PTC_TWISS and PTC_NORMAL can be used as guiding tools at a design stage, while tracking with PTC_TRACK can provide more reliable results
- Some automatizations for DA calculations and TBT analysis of PTC_TRACK data are desirable.
- It can be done by an inclusion into source code both algorithms used in MADX-input-scripts and external codes like SUSSIX by FS.